Affinity-based profiling of the adenosine receptors

Beerkens, B.L.H.

Chapter 6

Development of a Ligand-Directed Probe to Label the Adenosine A_{2B} Receptor

Bert L.H. Beerkens, Vasiliki Andrianopoulou, Rongfang Liu, Laura H. Heitman, Adriaan P. IJzerman and Daan van der Es.

Abstract

Ligand-directed labeling is a biochemical technique that utilizes chemical probes to selectively conjugate protein targets to a detection moiety. Contrary to other probe molecules, e.g. covalent ligands and affinity-based probes, the pharmacophore of a ligand-directed probe does not bind covalently to the binding pocket of the target protein. Instead, during the labeling event, the directing-ligand acts as a leaving group, allowing novel methods to study protein activity. Recently, ligand-directed probes have been reported for multiple types of GPCRs, such as the adenosine A_{2A} receptor, cannabinoid receptor type 2 and metabotropic glutamate receptor 1. In this work, we show the development and evaluation of the first ligand-directed probes for the adenosine A_{2B} receptor (A_{2B}AR). Two probe molecules were synthesized, pharmacologically characterized and biologically evaluated, of which one showed selective labeling of the A_{2B}AR in SDS-PAGE experiments. Interestingly, activation of the A_{2B}AR has been linked to the proliferation of cancer cells, among other hallmarks of cancer. Targeting the A_{2B}AR with ligand-directed probes might therefore offer new opportunities to investigate A_{2B}AR activity in cancer cell lines and tissues.

Introduction

The Adenosine A_{2B} Receptor (A_{2B}AR) is a class A G Protein-Coupled Receptor (GPCR) that is activated through binding of the endogenous signaling molecule adenosine.[1] The A_{2B}AR belongs to the subfamily of Adenosine Receptors (ARs), other members being the Adenosine A_1, A_{2A} and A_3 receptors (A_1AR, A_{2A}AR and A_3AR).[2] The ARs are widely expressed throughout the human body and activation of an individual receptor is strongly dependent on cell and tissue type. In recent years, the A_{2A}AR and A_{2B}AR have attracted attention due to their immunosuppressive role in the tumor micro-environment, leading to the proliferation of cancerous cells.[3–5] Antagonizing of the A_{2A} and A_{2B} receptors is therefore an interesting new strategy to target the tumor micro-environment. In fact, multiple clinical trials are currently ongoing using either selective or dual antagonists to target A_{2A} and A_{2B} receptors in cancer pathologies.[2]

The A_{2A}AR has been extensively studied: the receptor has been purified and crystallized as one of the first GPCRs and therefore became a prototypical GPCR for structure-based studies.[6] The A_{2B}AR on the other hand, has been relatively poorly studied. Due to the low affinity of adenosine for the A_{2B}AR, the receptor has been presumed to be of less importance in physiological and pathological conditions. This idea is changing however, as more and more research is being carried out to decipher the function of the A_{2B}AR. The increase in popularity is reflected in the recent elucidation of the A_{2B}AR three-dimensional structure,[7,8] as well as the surge of chemical tools to study the A_{2B}AR, such as PET tracers,[9–11] fluorescent ligands,[12–14] and covalent ligands.[15,16]

A wide variety of chemical and biological probe molecules has been developed to selectively target and detect GPCRs. Besides PET tracers, fluorescent ligands and covalent ligands, these include antibodies and affinity-based probes.[17–19] Of our particular interest are the affinity-based probes, that contain both an electrophilic and a reporter group on the same molecular scaffold. Together, these groups allow detection of GPCRs in an extended amount of biochemical assay types, as we recently have shown for the A_1AR, A_{2A}AR and A_3AR.[20–22] Next to affinity-based probes, also 'ligand-directed probes' are being developed as novel interrogators of GPCR function.

The idea behind ligand-directed chemistry, developed in the lab of Hamachi, is to selectively donate a functional group to a protein target of interest (POI) using mild electrophiles.[23–25] In brief, a high affinity ligand is conjugated to an electrophile and a reporter group, e.g. a fluorophore, biotin or a click handle. Upon binding of the ligand into the binding pocket of the POI, a nucleophilic amino acid residue in close proximity will attack the electrophilic group, leading to cleavage of the molecule and substitution of the reporter group onto the POI (Figure 1). A big advantage of this technique, as compared to fluorescent ligands and affinity-based probes, is that the ligand itself can leave the binding pocket after covalent donation of the reporter group. This allows new ways to study native proteins, e.g. by activating or blocking the POI after labeling by the probe.

Multiple GPCR-targeting ligand-directed probes have been developed over the past few years, e.g. for the bradykinin B_2 receptor (B_2R),[27] A_{2A}AR,[28,29] metabotropic glutamate receptor 1 ($mGlu_1$R),[30] μ opioid receptor (MOR),[31] cannabinoid receptor type 2 (CB_2R),[32] dopamine D1 receptor (D_1R),[33] and smoothened receptor (SMOR).[34] Most interestingly, one of the ligand-directed probes for the A_{2A}AR has been used to selectively label the A_2AR in a breast cancer cell line,[29] while other ligand-directed probes have already been used to label endogenous $mGlu_1$R and MOR in rodent brain slices.[30,31]

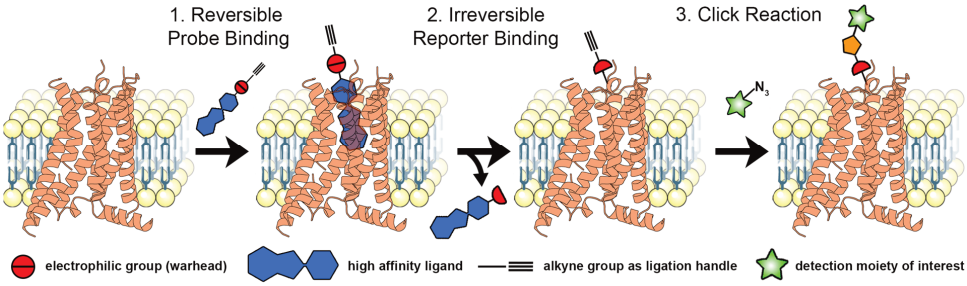

Figure 1. Labeling of GPCRs with ligand-directed probes. First, the probe binds to the receptor through its conjugated high affinity ligand. A nucleophilic amino acid residue then attacks the electrophilic group of the probe, inducing cleavage between the ligand and the reporter. The reporter group, e.g. a fluorophore, biotin or click handle, is now covalently bound to the receptor, while the ligand is allowed to leave the binding pocket (reversible mode of binding). This figure was partly created with Protein Imager,[26] using the structure of the A_{2B}AR (PDB: 8HDO).

In this study, we aim to expand the toolbox of ligand-directed probes for GPCRs by the development of A_{2B}AR-targeting probes. We show the synthesis and evaluation of ligand-directed probes for the A_{2B}AR, as well as labeling of the receptor in SDS-PAGE experiments. Altogether this will allow future investigations towards the detection of native A_{2B}AR in a multitude of biochemical assay types.

Results and Discussion

Design of the A_{2B}AR ligand-directed probes

In chapter 3 we reported on a xanthine-based compound, LUF7982, that covalently binds to the A_{2B}AR through a reaction of the attached fluorosulfonyl group with presumably a lysine residue (Scheme 1A).[15,16] The location of the fluorosulfonyl group on the xanthine scaffold thus is a valid position for the implementation of an electrophilic group for ligand-directed chemistry. Next to that, Tamura *et al.* have recently reported on the use of an *N*-acyl *N*-alkyl sulfonamide (NASA) group for the selective alkylation of a lysine residue on the folate receptor (Scheme 1B).[25] As the NASA group is based around the sulfonyl moiety, we envisioned that transforming the fluorosulfonyl group of LUF7982 into a NASA group would yield the first candidate A_{2B}AR ligand-directed probes (Scheme 1C). To increase the electrophilicity of the acyl group, Tamura *et al.* substituted various electron withdrawing groups onto the sulfonamide moiety (R_2-position),[25] of which the cyano group showed to be superior in terms of reaction kinetics. Therefore we also incorporated a cyano group into the design of our A_{2B}AR-targeting probes. For detection of the receptor, we chose to introduce an alkyne group at the R_3-position. This allows the usage of copper-catalyzed click chemistry to 'click' any reporter group of interest onto the alkylated receptor, without having to incorporate a bulky fluorophore in the design of the ligand.[35,36] Lastly, we varied the length of the alkyl linker between the NASA and the alkyne group, as linker length might influence affinity, reactivity and stability of the compounds. We have therefore synthesized probes containing either a 'short' 3-carbon linker, or a 'long' 8-carbon linker.

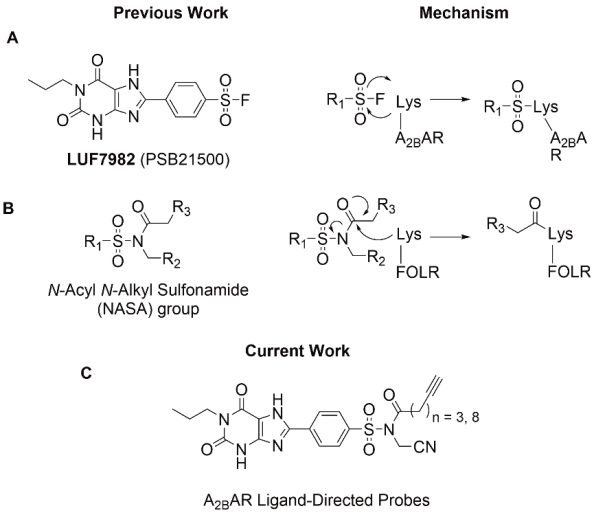

Scheme 1. (A) Molecular structure of the previously synthesized covalent antagonist LUF7982 (PSB21500) and its presumable mode of action at the A_{2B}AR; (B) Molecular structure of the *N*-acyl *N*-alkyl sulfonamide (NASA) group and its mode of action at the Folate Receptor (FOLR); (C) Design of the compounds synthesized in this work.

Synthesis of the A_{2B}AR ligand-directed probes

Synthesis of the two ligand-directed probes started with nitrosylated uracil **1**, synthesized as described in chapter 3.[15] The nitroso group was reduced with PtO_2 and H_2 (g) to obtain amine **2**,[37] which was used directly in a peptide coupling with 4-fluorosulfonyl benzoic acid and EDC·HCl to form amide **3** (Scheme 2). Trimethyl polyphosphate (PPSE) was used as condensating agent for the cyclization of uracil **3** to xanthine **4** (LUF7982),[38] and the fluorosulfonyl group was transformed into a sulfonamide group using aqueous ammonium hydroxide (28-30%). Sulfonamide **5** was used in the subsequent peptide couplings without further purifications and coupled to either 5-hexynoic acid or 10-undecynoic acid using EDC·HCl, DMAP and DIPEA to yield sulfonamides **6** and **8**. Up until this step crystallization was the purification method of preference, as the poor solubility of the xanthine compounds hindered purification by column chromatography. Lastly, the cyano moiety was introduced. Iodoacetonitrile, as used in other syntheses,[25] showed to be too reactive for this step, resulting in oversubstitution at the secondary amines of **6** and **8**. Therefore the milder bromoacetonitrile was used, yielding ligand-directed probes **7** (LUF8019) and **9** (LUF8023).

Stability of the synthesized compounds

Prior to investigating labelling of the A_{2B}AR by the synthesized ligand-directed probes, we investigated the stability of the compounds in aqueous buffer, as well as standard cell culture medium. Probes **7** (LUF8019) and **9** (LUF8023) were added to the buffer or medium, shaken and measured at different time points by LC-MS. Probes **7** (LUF8019) and **9** (LUF8023) were not susceptible towards hydrolysis, as only minor degradation was observed upon incubation in PBS buffer (Figure 2A). This corresponds to the previously observed hydrolytic stability of the NASA group.[25] However, upon incubation in cell culture medium, both **7** (LUF8019) and **9** (LUF8023) were eventually degraded to a compound with an m/z of 389 $[M+H]^+$ (Figure 2B), corresponding to the molecular weight of dealkylated product **10**. The observed bond cleavage is presumably the result of a reaction between the electrophilic NASA group and nucleophiles within the cell culture medium. Other teams have not reported on the susceptibility of the NASA

group towards nucleophiles other than the target proteins.[25,32] This might be due to a lack of investigation or differences in molecular structure. To prevent such unwanted side-reactions, we avoided the use of cell culture medium in all the subsequent experiments.

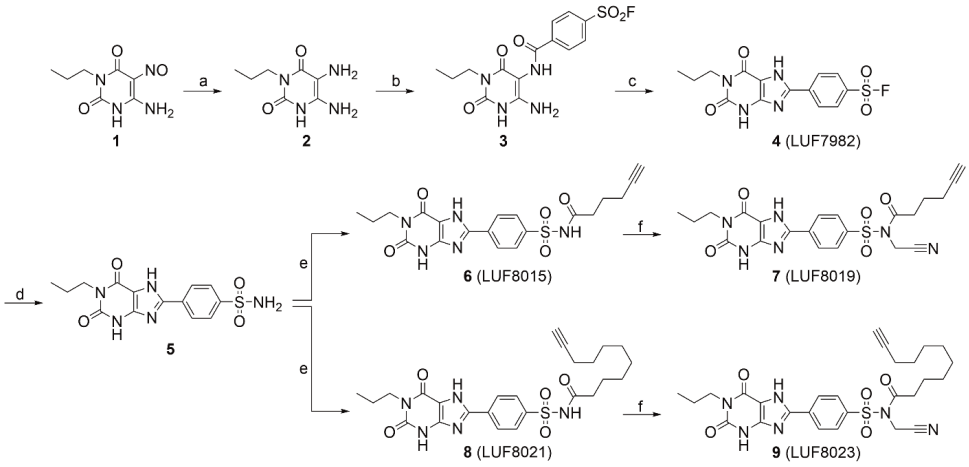

Scheme 2. (A) Molecular structures of the previously synthesized covalent A_{2B}AR antagonist LUF7982 (PSB21500), the NASA warhead, and the design of our ligand-directed probes. (B) Reagents and conditions. (a) PtO_2, H_2 (g), MeOH, RT, 1 h; (b) EDC·HCl, dry DMF, RT, 3 h, 62%; (c) PPSE, 180 °C, 3 h, 87%; (d) NH_4OH (28-30%), RT, 2 h, 75%; (e) EDC·HCl, respective benzoic acid, DMAP, DIPEA, dry DMF, RT, overnight, 41-64%; (f) Bromoacetonitrile, DIPEA, RT, 6-8 days, 12-41%.

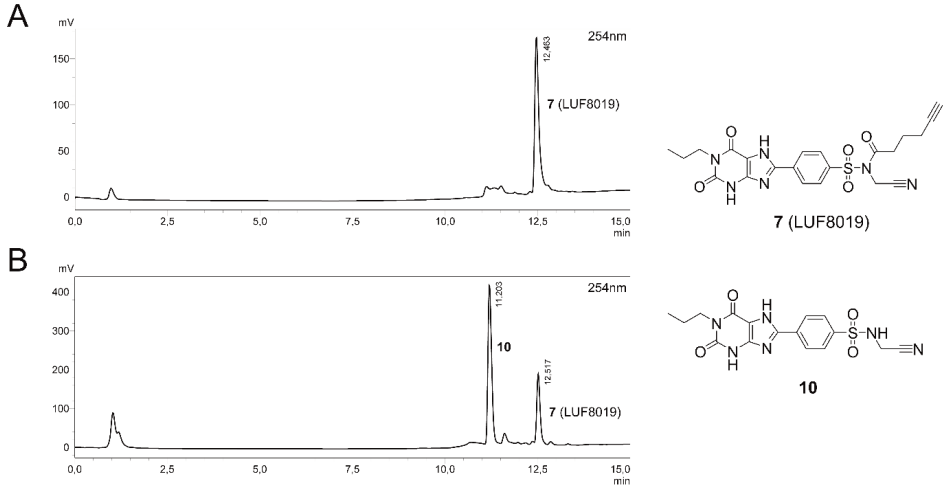

Figure 2 Investigation of probe stability in buffer and medium. Probe **7** (LUF8019) and **9** (LUF8023) were added to (A) PBS buffer or (B) DMEM/F12 medium containing 10% (v/v) newborn calf serum. Samples were shaken for 2 h at rt and afterwards measured by LC-MS. The LC-MS spectra of **7** (LUF8019) are shown as example.

Affinity towards the A_{2B}AR

First, to investigate the ability of the synthesized probes to bind to the A_{2B}AR, radioligand displacement assays were carried out. Control compounds **6** and **8**, lacking the cyano moiety, were included in these assays and a concentration range from 0.1 to 1000 nM of probe was chosen. Two different conditions were investigated: with and without 4 hours of pre-incubation between A_{2B}AR and ligand, prior to addition of radioligand. Using this assay setup, we have observed in chapters 3,4 and 5 that a time-dependent increase in affinity (pre-0h to pre-4h) is a strong indication of a covalent mode of binding.[15,20,39] All synthesized probes showed a decent to good affinity towards the A_{2B}AR, ranging from sub-micromolar (**6**) to double- (**7**-**8**) and single- (**9**) digit nanomolar values at pre-0h (Table 1). Of the four ligands, only **9** (LUF8023) showed to bind with similar strong affinity as **4** (LUF7982). However, contrary to covalent antagonist **4** (LUF7982), none of the synthesized ligands showed a significant time-dependent increase in affinity upon four hours of pre-incubation. This corresponds to the general idea of the ligand-directed probes, being able to leave the binding pocket after donation of the reporter group. Interestingly, compound **9** (LUF8023) showed a decrease in affinity upon 4 hours of pre-incubation. There are multiple possible explanations for this, for example, **9** (LUF8023) might have a higher affinity towards the A_{2B}AR than its cleaved product (**10**), or the donated alkyl group might influence binding of the ligand or radioligand to the A_{2B}AR. To investigate subtype selectivity of the synthesized probes, single point radioligand displacement experiments were carried out on the other adenosine receptors (Table 1). Most of the synthesized compounds showed poor binding to the other ARs (<50% displacement), while only control compound **8** (LUF8021) showed a strong displacement (82%) at the A_1AR. The actual ligand-directed probes **7** (LUF8019) and **9** (LUF8023) thus are selective towards the A_{2B}AR over the other ARs.

Table 1. Radioligand displacement of the synthesized ligand-directed probes on the four adenosine receptors.

	pK_i (pre-0h)[a]	pK_i (pre-4h)[b]	Displacement at 1 µM (%)		
Compound	A_{2B}AR	A_{2B}AR	A_1AR[c]	A_{2A}AR[d]	A_3AR[e]
4 (LUF7982)[f]	8.10 ± 0.06	9.17 ± 0.12**	29 (28, 30)	52 (59, 46)	7 (11, 3)
6 (LUF8015)	6.44 ± 0.06	6.60 ± 0.10	19 (21, 17)	9 (6, 12)	-5 (-8, -2)
7 (LUF8019)	7.31 ± 0.05	7.44 ± 0.12	34 (30, 38)	40 (35, 45)	-2 (-8, 5)
8 (LUF8021)	7.26 ± 0.07	7.51 ± 0.06	82 (82, 81)	0 (-3, 3)	6 (-2, 14)
9 (LUF8023)	8.22 ± 0.10	7.75 ± 0.08*	46 (46, 46)	27 (15, 38)	-9 (-14, -3)

[a] Apparent affinity determined from displacement of specific [^{3}H]PSB-603 binding on CHO-spap cell membranes stably expressing the hA_{2B}AR at 25 °C after 0.5 h of co-incubating probe and radioligand. [b] Apparent affinity determined from displacement of specific [^{3}H]PSB-603 binding on CHO-spap cell membranes stably expressing the hA_{2B}AR at 25 °C after 4 h of pre-incubation with the respective probe, followed by an additional 0.5 h of co-incubation with radioligand. [c] % specific [^{3}H]DPCPX displacement by the respective probe on CHO cell membranes stably expressing the hA_1AR at 25 °C after 0.5 h of co-incubating probe and radioligand; [d] % specific [^{3}H]ZM241385 displacement by the respective probe on HEK293 cell membranes stably expressing the hA_{2A}AR at 25 °C after 0.5 h of co-incubating probe and radioligand; [e] % specific [^{3}H]PSB11 displacement by the respective probe on CHO cell membranes stably expressing hA_3AR at 25 °C after 0.5 h of co-incubating probe and radioligand. [f] Values obtained from previous experiments.[15] Data represent the mean ± SEM of three individual experiments performed in duplicate [a-b] or the mean of two individual experiments performed in duplicate [c-e]. *$p < 0.05$, **$p < 0.01$ compared to the pKi values at pre-0h, determined by a two-tailed unpaired Student's t-test.

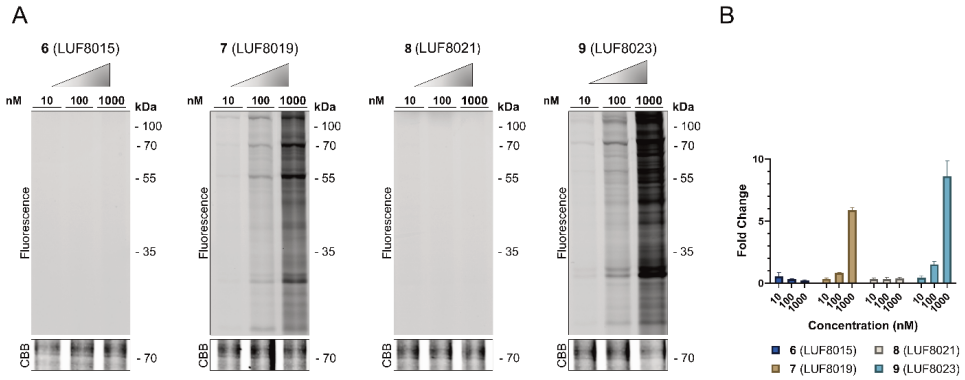

Figure 3 Ligand-directed labelling of the respective ligand-directed probes in CHO-A_{2B}AR-spap membrane fractions. CHO-spap membrane fractions with stable expression of the A_{2B}AR were incubated for 2 h with probes **6** (LUF8015), **7** (LUF8019), **8** (LUF8021) or **9** (LUF8023). Probe-bound proteins were clicked to Cy5-N_3, denatured and resolved by SDS-PAGE. Gels were imaged by in-gel fluorescence. Coomassie Brilliant Blue (CBB) staining was used as loading control. (B) Quantification of the lane intensities. The lane intensities were taken and corrected for the observed amount of protein per lane upon Coomassie staining. The PageRuler Plus ladder (not shown) was used as reference lane and fold changes were calculated relative to this lane (adjusted intensity lane/adjusted intensity reference lane). The mean values ± SEM of three individual experiments are shown.

Labelling of the A_{2B}AR in SDS-PAGE experiments

Finally, the probes were evaluated for their ability to label the A_{2B}AR in SDS-PAGE experiments. In an initial screen probes **7** (LUF8019) and **9** (LUF8023) as well as control compounds **6** (LUF8015) and **8** (LUF8021) were investigated for their ability to label proteins in membrane fractions derived from A_{2B}AR-expressing Chinese hamster ovary (CHO) cells. The membrane fractions were incubated with 10, 100 or 1000 nM of the respective probes, clicked to a Cy5 fluorophore, denatured and resolved by SDS-PAGE. Ligand-directed probes **7** (LUF8019) and **9** (LUF8023) labelled multiple proteins at concentrations ≥10 nM (Figure 3A), while no labelling was observed for control compounds **6** (LUF8015) and **8** (LUF8021), indicating that the cyano substitution is necessary to enhance the electrophilicity of the *N*-acyl group. Additionally, probes **7** (LUF8019) and **9** (LUF8023) show unwanted off-target labelling. In case of the electrophilic probes for the A_1AR and the A_3AR (chapters 4 and 5), we also observed off-target labelling in membrane-derived samples, however not in cellular assays.[20,22] We therefore moved towards cellular assays in our endeavors to label the A_{2B}AR. For these experiments, we chose a probe concentration of 100 nM as a balance between a low (10 nM) and high (1000 nM) degree of protein labeling (Figure 3B).

Live CHO cells with and without stable expression of the A_{2B}AR were first pre-incubated with 1 µM competing ligand and then incubated with 100 nM of ligand-directed probe **7** (LUF8019) or **9** (LUF8023) in Hank's Balanced Salt Solution (HBSS). Non-bound probe was washed away and membrane fractions were collected. Probe-bound proteins were clicked to Cy5-N_3. Samples were then denatured, loaded on SDS-PAGE and the gels were visualized using in-gel fluorescence. Probe **7** (LUF8019) showed clear labelling of one protein, visible as a smear at about 60 kDa (Figure 4A). This protein was absent in the control lanes (without A_{2B}AR or probe) and therefore presumably the A_{2B}AR. Removal of N-glycans through PNGase showed a strong reduction in molecular weight of the observed band, towards a molecular weight that more closely resembles the weight of the A_{2B}AR (36 kDa). A similar pattern of bands has also been observed in western blot experiments and characterized as being the A_{2B}AR.[40–42] Upon pre-incubation with covalent antagonist **4** (LUF7982) the observed fluorescent signal was

significantly reduced (Figure 4B). The partial agonist BAY60-6583 and antagonist PSB1115 however did not significantly reduce A_{2B}AR labelling by probe **7** (LUF8019). Presumably their reversible mode of binding, in combination with sub-micromolar affinities for the A_{2B}AR (212 and 53 nM respectively)[43,44] allow occasional binding of the ligand-directed probe and subsequent labeling of the receptor. Contrary to probe **7** (LUF8019), ligand-directed probe **9** (LUF8023) did not show any specific labelling of the A_{2B}AR (Figure 4C). An increased reactivity of the probe, resulting in faster cleavage of the NASA group, may be the reason for this observation.

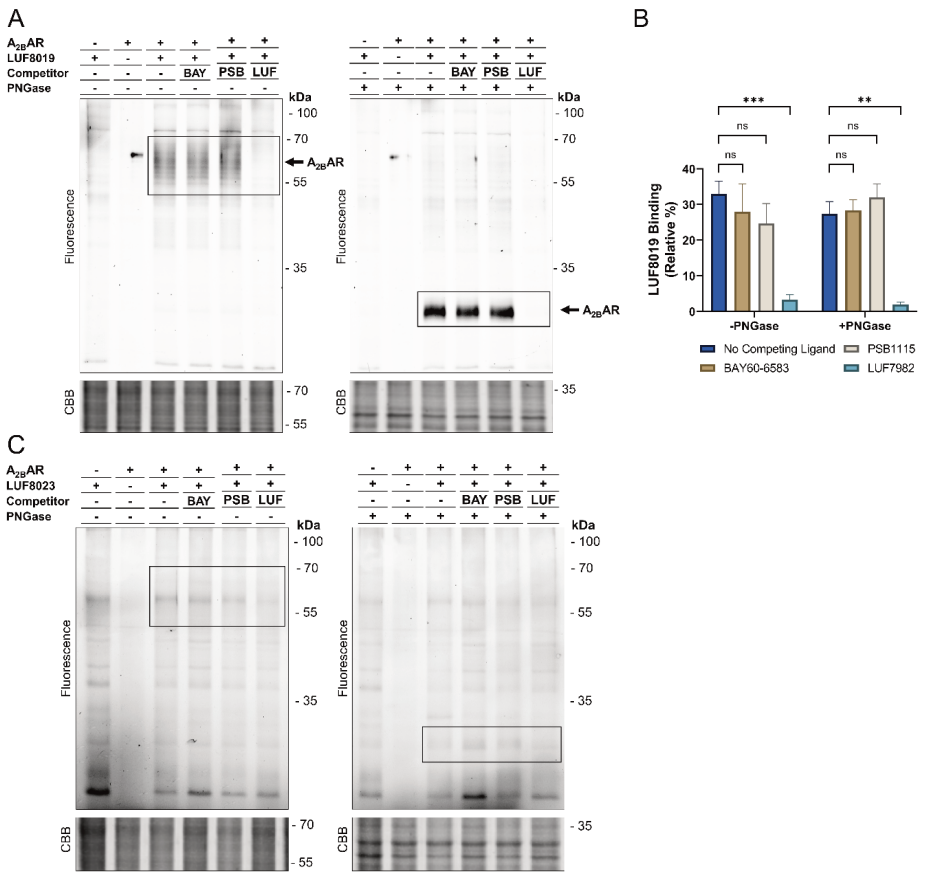

Figure 4 Ligand-directed labelling of the A_{2B}AR in and live CHO cells. CHO-spap cells with or without (lane 1) stable expression of the A_{2B}AR were pre-incubated for 30 min with 1 µM antagonist in medium (BAY60-6583 (BAY), PSB1115 (PSB) or **4** (LUF7982; LUF) and subsequently incubated for 2 h with 100 nM probe (LUF8019 or LUF8023) in HBSS. Cells were washed with PBS and membranes were collected. N-glycans were removed using PNGase (5 U) and alkyne moieties were clicked to 1 µM Cy5-N_3. The samples were then denatured using Laemmli buffer and resolved by SDS-PAGE. Gels were imaged by in-gel fluorescence. Coomassie Brilliant Blue (CBB) staining was used as loading control. (A) Protein labeling by LUF8019. (B) Quantification of A_{2B}AR labelling by LUF8019. The band intensities were taken and corrected for the observed amount of protein per lane upon Coomassie staining. The band at 55 kDa of the PageRuler Plus ladder (not shown) was set to 100% for each gel and band intensities were calculated relative to this band. The mean values ± SEM of three individual experiments are shown. Significance was calculated using a two-way ANOVA test with multiple comparisons; (C) Protein labeling by LUF8023. All shown gels are representatives of the experiments performed with n=3.

Altogether, of the two synthesized ligand-directed probes **7** (LUF8019) was able to selectively label the A_{2B}AR in CHO cells. Looking at the ligand-directed probes developed for the A_{2A}AR, slight differences in molecular structure already seem to cause different modes of binding. Probes bearing a 2-nitrophenyl ester fully blocked the orthosteric binding pocket in radioligand displacement assays, likely occupying the A_{2A}AR in a covalent fashion.[28] On the contrary, a 2-fluorophenyl ester-containing probe successfully labelled endogenous A_{2A}AR.[29] The latter probe was studied in functional assays to measure receptor activation after labelling. Activation of the A_{2A}AR was achieved after 16 h of incubation, indicating full dissociation of the released ligand. The 2-fluorophenyl ester probe thus seems to bind and label the A_{2A}AR in a ligand-directed manner, although with slow binding kinetics. To overcome such long incubation times, the NASA group has been developed and implemented as electrophile with fast kinetics.[25] This strategy yielded successful ligand-directed probes for the CB_2R, as shown in flow cytometry and confocal microscopy experiments.[32] However, dissociation of the released ligands from their binding pockets has not been confirmed in these studies. Such experiments would therefore be a first step towards further characterization of the herein presented ligand-directed probes for the A_{2B}AR.

Conclusion

In summary, we show here the development of the first ligand-directed probe for the A_{2B}AR. Two probes and two control compounds were synthesized, all showing a good affinity and selectivity towards the A_{2B}AR in radioligand displacement assays. Both ligand-directed probes labelled proteins upon incubation in CHO membrane fractions, while only one of the two probes, **7** (LUF8019), showed specific labelling of the A_{2B}AR in live CHO cells. Labelling of the A_{2B}AR could be prevented by pre-incubation with a covalent antagonist, but not by reversible A_{2B}AR ligands. Changing the assay conditions, e.g. by increasing the amount of competing ligand, increasing the competing ligand incubation time or decreasing the probe incubation time, might lead to a stronger competition by the reversible ligands for the A_{2B}AR binding pocket. Probe **9** (LUF8023) on the other hand, did not label the A_{2B}AR in live CHO cells. Altogether, this data suggests ligand-directed probe **7** (LUF8019) to be a valid tool to “tag” the A_{2B}AR.

The ability to click a fluorophore or a biotin moiety onto the receptor, together with the ability of the ligand to dissociate after donation of the reporter group, allows the investigation of agonist-induced activation of the receptor. For example, internalization and subcellar localization of the receptor might be studied with aid of ligand-directed probe **7** (LUF8019). We are currently investigating the optimal assay conditions that allow us to perform such experiments with probe **7** (LUF8019).

Experimental

Chemistry

General

All reactions were performed using commercially available chemicals and solvents, purchased via Sigma-Aldrich (Merck), VWR chemicals and Thermo Scientific. All reactions were carried out under an N_2 atmosphere and at room temperature, unless noted otherwise. Thin layer chromatography (TLC) was carried out using TLC Silica Gel 60 F254 (Merck) and visualized using UV irradiation at wavelengths of 254 and 366 nM. ^{1}H, ^{13}C and ^{19}F NMR spectra were recorded on a Bruker AV-400 (400 MHz) or Bruker AV-500 (500 MHz) spectrometer. Chemical shift values are reported in parts per million (ppm) and designated by δ. Tetramethylsilane or solvent resonance was used as internal standard. Coupling constants (J) are reported in Hertz (Hz) and multiplicities are indicated by s (singlet), bs (broad singlet), d (doublet), t (triplet), td (triplet of doublets), p (pentuplet), h (hexuplet) or m (multiplet). Compound purity was determined by HPLC-MS, using a LCMS-2020 system coupled to a Gemini® 3 µm C18 110Å column (50 x 3 mm). Samples were dissolved in H_2O:MeCN:*t*-BuOH 1:1:1, injected onto the column and eluted with a gradient of H_2O:MeCN 9:1 + 1% formic acid to H_2O:MeCN 1:9 + 1% formic acid over the course of 15 minutes. High-resolution mass spectrometry (HRMS) measurements were done on a X500R QTOF mass spectrometer (SCIEX).

Synthesis of ligand-directed probes

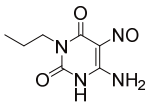

6-Amino-5-nitroso-3-propylpyrimidine-2,4(1H,3H)-dione (1)
Compound **1** was synthesized as described in chapter 3.

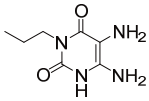

5,6-Diamino-3-propylpyrimidine-2,4(1*H*,3*H*)-dione (2)[37]
Uracil derivative **1** (2.00 g, 10.09 mmol, 1.0 eq) was dissolved in MeOH (80 mL) and PtO_2 (40 mg) was added to the flask. The flask was flushed once with N_2 (g), twice with H_2 (g) and then kept under H_2 (g) for hydrogenation. After 1 h, a gray solid was formed. DCM (500 mL) was added to the flask and the mixture was filtered over Celite. The filtrate was concentrated under reduced pressure to yield quantitative **2** as orange/brown solid. To prevent degradation, compound **2** was used in the next steps without further purifications.

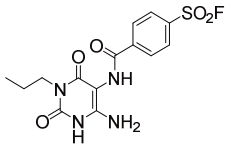

4-((6-Amino-2,4-dioxo-3-propyl-1,2,3,4-tetrahydropyrimidin-5-yl)carbamoyl)benzenesulfonyl fluoride (3)

EDC·HCl (2.01 g, 10,5 mmol, 1.2 eq) was added to a solution of diamine **2** (1.97 g, 9.63 mmol, 1.1 eq) in dry DMF (44 mL). After stirring for 3 h, EtOAc (250 mL) was added and the organic layer was washed with H_2O (250 mL), dried over $MgSO_4$, filtered and concentrated under reduced pressure. The compound was recrystallized overnight using MeOH/EtOAc to yield **3** as an orange solid (2.30 g, 6.20 mmol, 62%). **^{1}H NMR** (500 MHz, $(CD_3)_2SO$) δ [ppm] = 10.55 (s, 1H), 9.30 (s, 1H), 8.27 (s, 4H), 6.26 (s, 2H), 3.66 (t, *J* = 7.3 Hz, 2H), 1.50 (h, *J* = 7.5 Hz, 2H), 0.84 (t, *J* = 7.5 Hz, 3H). **^{19}F NMR** (471 MHz, $(CD_3)_2SO$) δ [ppm] = 66.0.

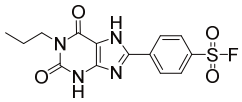

4-(2,6-Dioxo-1-propyl-2,3,6,7-tetrahydro-1*H*-purin-8-yl)benzenesulfonyl fluoride (4)

Trimethylsilyl polyphosphate (PPSE) (31 mL) was added to compound **3** (2.30 g, 6.20 mmol, 1.0 eq) and the mixture was brought to 180 °C under reflux conditions. The formed solution was stirred for 3 h and afterwards cooled down to room temperature, followed by cooling on ice. MeOH (200 mL) was added and the mixture was stirred for 5 min. The mixture was filtered and the residue was washed with MeOH (100 mL), collected and dried under vacuum to yield **4** (1.90 g, 5.39 mmol, 87%) as an off-white powder. **^{1}H NMR** (500 MHz, $(CD_3)_2SO$) δ [ppm] = 14.24 (s, 1H), 12.04 (s, 1H), 8.44 (d, *J* = 8.7 Hz, 2H), 8.28 (d, *J* = 8.7 Hz, 2H), 3.91 – 3.77 (m, 2H), 1.58 (h, *J* = 7.5 Hz, 2H), 0.88 (t, *J* = 7.5 Hz, 3H). **^{19}F NMR** (471 MHz, $(CD_3)_2SO$) δ [ppm] = 66.2.

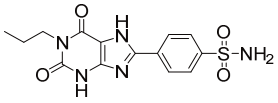

4-(2,6-Dioxo-1-propyl-2,3,6,7-tetrahydro-1*H*-purin-8-yl)benzenesulfonamide (5)

Sulfonyl fluoride **4** (1.6 g, 4.54 mmol, 1.0 eq) was dissolved in 28-30% ammonia solution (23 mL) and stirred for 2 h. The reaction mixture was then quenched and acidified by dropwise addition of 6 M HCl (60 mL). The product was crystallized overnight and the residue was collected by vacuum filtration. To remove impurities, the residue was dissolved in 0.5 M NaOH (75 mL) and the aqueous mixture was washed using 100 mL of 5% MeOH in $CHCl_3$. The pH was then brought to ~2 using 6 M HCl and the product was allowed to crystallize overnight. The residue was collected by vacuum filtration and dried under vacuum to yield **5** (1.19 g, 3.40 mmol, 75 %) as a purple solid, which was used in the next steps without further purification. **^{1}H NMR** (400 MHz, $(CD_3)_2SO$) δ [ppm] = 11.78 (bs, 1H), 8.21 (d, *J* = 8.6 Hz, 2H), 7.87 (d, *J* = 8.3 Hz, 2H), 7.41 (s, 2H), 3.81 (t, *J* = 7.5 Hz, 2H), 1.56 (h, *J* = 7.6 Hz, 2H), 0.87 (t, *J* = 7.4 Hz, 3H).

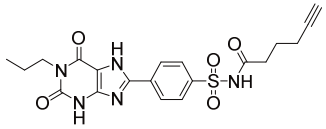

***N*-((4-(2,6-Dioxo-1-propyl-2,3,6,7-tetrahydro-1*H*-purin-8-yl)phenyl)sulfonyl)hex-5-ynamide (6) (LUF8015)**

5-hexynoic acid (98 µL, 0.89 mmol, 1.6 eq), EDC·HCl (316 mg, 1.65 mmol, 3.0 eq), DMAP (20 mg, 0.17 mmol, 0.3 eq) and DIPEA (290 µL, 1.66 mmol, 3.0 eq) were added to a solution of sulfonamide **5** (192 mg, 0.55 mmol,1.0 eq) in dry DMF (6 mL) and the mixture was stirred overnight. EtOAc (50 mL) was added and the organic layer was washed with H_2O (3 x 50 mL). As the product resided in the aqueous layer, the aqueous layers were combined and the pH was brought to ~2 using 6 M HCl. The product was allowed to crystallize overnight and collected by vacuum filtration. The filtrate was recrystallized and the second residue was collected by vacuum filtration. The residues were combined and purified using column chromatography (DCM:MeOH 98:2→93:7) to yield **6** (101 mg, 0.03 mmol, 41%) as an off-white solid. **^{1}H NMR** (500 MHz, $(CD_3)_2SO$) δ [ppm] = 14.03 (s, 1H), 11.99 (s, 1H), 8.28 (d, *J* = 8.7 Hz, 2H), 8.00 (d, *J* = 8.7 Hz, 2H), 3.82 (t, *J* = 7.3 Hz, 2H), 2.76 (t, *J* = 2.6 Hz, 1H), 2.32 (t, *J* = 7.4 Hz, 2H), 2.08 (td, *J* = 7.1, 2.7 Hz, 2H), 1.61 – 1.53 (m, 4H), 0.88 (t, *J* = 7.4 Hz, 3H). **^{13}C NMR** (126 MHz, DMSO) δ 172.2, 155.5, 151.5, 148.6, 148.1, 141.0, 133.7, 128.7, 127.2, 109.1, 84.2, 72.3, 42.0, 34.9, 23.4, 21.4, 17.5, 11.7. **HRMS** (ESI, m/z): $[M+H]^+$, calculated: 444.1336, found: 444.1308. **HPLC** 97%, RT 8.797 min.

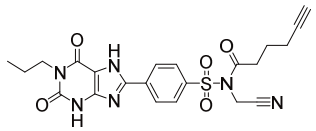

***N*-(Cyanomethyl)-*N*-((4-(2,6-dioxo-1-propyl-2,3,6,7-tetrahydro-1*H*-purin-8-yl)phenyl)sulfonyl)hex-5-ynamide (7) (LUF8019)**

Bromoacetonitrile (8 µL, 0.11 mmol,1.2 eq) was added to a solution of **6** (43 mg, 0.10 mmol, 1.0 eq) in dry DMF (3 mL) and the mixture was stirred overnight. A small conversion of starting material was observed and therefore extra bromoacetonitrile (4 µL, 0.06 mmol, 0.05 eq) was added. The mixture was further stirred for 8 days during which DIPEA (14 µL, 0.08 mmol, 0.8 eq) was added gradually. The reaction was then stopped to prevent overalkylation. EtOAc (50 mL) was added and the organic layer was washed with H_2O (3 x 50 mL), dried using $MgSO_4$, filtered and concentrated under reduced pressure. The residue was purified using column chromatography (DCM: MeOH 99.5:0.5→ 97.5:2.5) to yield **7** (20 mg, 0.04 mmol, 41%) as white solid. **^{1}H NMR** (500 MHz, $(CD_3)_2SO$) δ [ppm] = 14.10 (s, 1H), 12.01 (s, 1H), 8.35 (d, *J* = 8.6 Hz, 2H), 8.16 (d, *J* = 8.7 Hz, 2H), 4.98 (s, 2H), 3.82 (t, *J* = 7.4 Hz, 2H), 2.81 (t, *J* = 7.2 Hz, 2H), 2.77 (t, *J* = 2.6 Hz, 1H), 2.16 (td, *J* = 7.0, 2.7 Hz, 2H), 1.65 (p, *J* = 7.1 Hz, 2H), 1.57 (h, *J* = 7.4 Hz, 3H), 0.88 (t, *J* = 7.4 Hz, 3H). **^{13}C NMR** (126 MHz, $(CD_3)_2SO$) δ [ppm] = 172.2, 155.5, 151.5, 148.1, 148.1, 138.7, 134.9, 129.1, 127.6, 116.9, 109.4, 84.0, 72.5, 42.1, 34.7, 34.5, 23.4, 21.4, 17.3, 11.7. **HRMS** (ESI, m/z): $[M+H]^+$, calculated: 483.1445, found: 483.1423. **HPLC** 96%, RT 9.721 min.

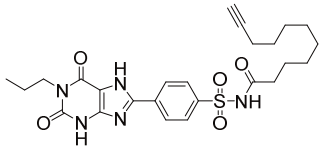

***N*-((4-(2,6-Dioxo-1-propyl-2,3,6,7-tetrahydro-1*H*-purin-8-yl)phenyl)sulfonyl)undec-10-ynamide (8) (LUF8021)**

10-Undecynoic acid (328 mg, 1.80 mmol,1.6 eq), EDC·HCl (656 mg, 3 mmol, 3 eq), DMAP (42 mg, 0.34 mmol, 0.3 eq) and DIPEA (600 µL, 3.44 mmol, 3.0 eq) were added to a solution of **5** (400 mg, 1.14 mmol, 1.0 eq) in dry DMF (12 mL) and the mixture was stirred overnight. EtOAC (100 mL) was then added and the organic layer was extracted with H_2O (3 x 100 mL). As the product resided in the aqueous layer, the aqueous layers were combined and the pH was brought to ~2 using 6 M HCl. The product was allowed to crystallize overnight and was collected by filtration. The product was further purified by recrystallization in a 1:4 mixture of H_2O:EtOAc to yield compound **8** as a pink-white solid (376 mg, 0.73 mmol, 64%). **^{1}H NMR** (400 MHz, $(CD_3)_2SO$) δ [ppm] = 14.05 (s, 1H), 12.16 (s, 1H), 11.99 (s, 1H), 8.29 (d, *J* = 8.6 Hz, 2H), 8.00 (d, *J* = 8.6 Hz, 2H), 3.82 (t, *J* = 7.4 Hz, 2H), 2.69 (t, *J* = 2.6 Hz, 1H), 2.20 (t, *J* = 7.2 Hz, 2H), 2.06 (td, *J* = 7.0, 2.7 Hz, 2H), 1.57 (h, *J* = 7.5 Hz, 2H), 1.43 – 1.28 (m, 4H), 1.27 – 1.18 (m, 2H), 1.17 – 1.02 (m, 6H), 0.88 (t, *J* = 7.4 Hz, 3H). **^{13}C NMR** (101 MHz, $(CD_3)_2SO$) δ [ppm] = 172.3, 155.4, 151.4, 148.4, 148.1, 140.5, 133.8, 128.7, 127.1, 109.0, 84.9, 71.5, 42.0, 35.8, 29.0, 28.8, 28.6, 28.5, 28.4, 24.4, 21.3, 18.1, 11.7. **HRMS** (ESI, m/z): $[M+H]^+$, calculated: 514.2119, found: 514.2089. **HPLC** 100%, RT 10.459 min.

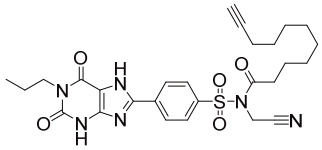

***N*-(Cyanomethyl)-*N*-((4-(2,6-dioxo-1-propyl-2,3,6,7-tetrahydro-1*H*-purin-8-yl)phenyl)sulfonyl)undec-10-ynamide (9) (LUF8023)**

Bromoacetonitrile (21 µL, 0.30 mmol, 1.2 eq) was added to a solution of **8** (130 mg, 0.25 mmol, 1.0 eq) in dry DMF (8 mL). DIPEA (14 µL, 0.08 mmol, 0.3 eq) was added gradually over a period of six days. The reaction was then stopped to prevent overalkylation. EtOAc (100 mL) was added and the organic layer was washed using H_2O (3 x 100mL), dried over $MgSO_4$ and concentrated under reduced pressure. The residue was purified using column chromatography (DCM: MeOH 99.5:0.5→98:2) to yield **9** (16 mg, 0.02 mmol, 12%) as a white solid. **^{1}H NMR** (500 MHz, $(CD_3)_2SO$) δ [ppm] = 14.11 (s, 1H), 12.00 (s, 1H), 8.35 (d, *J* = 8.8 Hz, 2H), 8.15 (d, *J* = 8.7 Hz, 2H), 5.00 (s, 2H), 3.82 (t, *J* = 7.3 Hz, 2H), 2.67 (t, *J* = 2.7 Hz, 1H), 2.64 (t, *J* = 7.2 Hz, 2H), 2.06 (td, *J* = 7.0, 2.7 Hz, 2H), 1.58 (h, *J* = 7.4 Hz, 2H), 1.47 – 1.40 (m, 2H), 1.38 – 1.29 (m, 2H), 1.25 – 1.20 (m, 2H), 1.17 – 1.09 (m, 6H), 0.88 (t, *J* = 7.5 Hz, 3H). **^{13}C NMR** (126 MHz, $(CD_3)_2SO$) δ [ppm] = 172.7, 155.5, 151.5, 148.1, 148.0, 139.0, 134.8, 129.1, 127.5, 117.0, 109.3, 85.0, 71.5, 42.1, 35.6, 34.5, 29.0, 28.8, 28.6, 28.5, 28.4, 24.4, 21.4, 18.1, 11.7. **HRMS** (ESI, m/z): $[M+H]^+$, calculated: 553.2228, found: 553.2218. **HPLC** 98%, RT 11.300 min.

Biology

Materials

[^{3}H]PSB-603 (specific activity 79 Ci/mmol) was purchased from Quotient Bioresearch, [^{3}H]DPCPX, (specific activity 137 Ci/mmol) and [^{3}H]-ZM241385 (specific activity 50 Ci/mmol) were purchased from ARC, Inc. and [^{3}H]PSB-11 (specific activity 56 Ci/mmol) was kindly donated by Prof. C.E. Müller (University of Bonn, Germany). 5'-(N-Ethylcarboxamido)adenosine (NECA), N^6-Cyclopentyladenosine (CPA), EDTA-free protease inhibitor cocktail (cat# P8340) and all click reagents $CuSO_4$, (+)-sodium L-ascorbate (NaAsc), Tris((1-hydroxy-propyl-1H-1,2,3-triazol-4-yl)methyl)amine (THPTA) and Cy5-N_3, were purchased from Sigma-Aldrich (Merck). ZM241385 was a gift of Dr. S.M. Poucher (Astra Zeneca, Manchester, UK) and CGS21680 was purchased from Ascent Scientific. PSB 1115 potassium salt was purchased from Tocris Bioscience and BAY60-6583 and LUF7982 were synthesized in-house as reported before.[15] Adenosine Deaminase (ADA) was purchased from Sigma-Aldrich (Merck) and PNGase F (10 u/µL, cat# V4831) was purchased from Promega. Laemmli buffer was purchased from Bio-Rad and Hank Buffered Saline Solution (HBSS) (cat# 1402550) was purchased from Thermo Fischer. All other reagents were purchased from standard commercial sources and of analytical grade.

Stability assays

5 µL of a 7.5 mM stock solution of probe was added to an LC-MS vial containing 95 µL of PBS buffer or CHO-hA_{2B}AR-spap culture medium (DMEM/F12 1:1, 10% (v/v) Newborn Calf Serum (NCS), 100 mg/mL penicillin/streptomycin, 1 mg/mL G418 and 0.4 mg/mL hygromycin). The samples were constantly shaken at 1000 rpm (rt or 37 °C) to prevent the probes from crystallizing. Samples were measured by LC-MS after 2 h of incubation, using the method described above.

Cell culture and membrane preparation

Chinese Hamster Ovary (CHO)-spap cells stably expressing the human adenosine A_{2B} receptor (CHO-spap-hA_{2B}AR) were kindly provided by S.J. Dowell (GlaxoSmithKline, Stevenage, UK), CHO cells stably expressing the human adenosine A_1 receptor (CHO-hA_1AR) were kindly provided by Prof. S.J. Hill (Nottingham, UK), Human Embryonic Kidney (HEK) 293 cells stably expressing the human adenosine A_{2A} receptor (HEK293-hA_{2A}AR) were kindly provided by Dr. J. Wang (Biogen, Cambridge, Massachusetts USA) and CHO cells stably expressing the human adenosine A_3 receptor (CHO-hA_3AR) were kindly provided by Dr. K.N. Klotz (University of Würzburg, Germany). All cells were cultured and membranes were prepared as reported before.[45]

Radioligand displacement assays

Full curve radioligand displacement experiments using CHO-hA_{2B}AR-spap membranes and single point displacement assays using CHO-hA_1AR, HEK293-hA_{2A}AR and CHO-hA_3AR membranes were carried out as previously reported.[15] Data was analyzed using GraphPad Prism 9.0 (Graphpad Software Inc., San Diego, California USA). IC_{50} values were obtained by non-linear regression curve fitting and converted to pIC_{50} values using the Cheng-Prusoff equation.[46] The KD values of 1.7 nM of [^{3}H]PSB-603 at CHO-spap-hA_{2B}AR membranes and 1.6 nM of [^{3}H]DPCPX at CHO-hA_1AR membranes were taken from previous experiments.[47,48] The KD values of 1.0 nM of [^{3}H]ZM241385 at HEK293-hA_{2A}AR membranes and 17.3 nM of [^{3}H]PSB11 at CHO-hA_3AR membranes were taken from in-house determinations. All pK_i values shown are mean values ± SEM of three individual experiments performed in duplicate.

Single point displacement values are the mean percentages of two experiments performed in duplicate. Statistical analysis was performed using a two-tailed unpaired student's T-test.

SDS-PAGE using CHO-hA_{2B}AR-spap membrane fractions

CHO-hA_{2B}AR-spap membrane fractions were collected as previously reported.[45] Protease inhibitor cocktail (1:100) was added, the membrane fractions were diluted to a concentration of 1 mg/mL and 19 µL was taken per sample. 1 µL of probe LUF8015, LUF8019, LUF8021 or LUF8023 (final concentration: 100 nM) was added and the samples were incubated for 1 h at rt. Click mix was freshly prepared by combining 5 parts 100 mM $CuSO_4$, 3 parts 1 M NaAsc, 1 part 100 mM THPTA and 1 part 100 µM Cy5-N_3. 2.22 µL of the prepared click mix was added per sample and the samples were incubated for 1 h at rt. Proteins were denatured by addition of 7.41 µL of Laemmli buffer (x4) and incubation for at least 1 h at rt. The samples were then loaded on gel (12.5% acrylamide) and run (180 V, 100 min). Gels were imaged on a Bio-Rad Universal Hood III using in-gel fluorescence. Pageruler prestained protein ladder was used as molecular weight marker. Coomassie Brilliant Blue (CBB) staining was carried out as control.

SDS-PAGE using live CHO-hA_{2B}AR-spap cells

CHO-hA_{2B}AR-spap cells were cultured as previously reported.[45] Upon reaching ~90% confluency, medium was removed and competing ligand PSB1115, BAY60-6583 or LUF7982 (final concentration: 1 µM) or 1% DMSO (vehicle) in medium was added, followed by a 30 min incubation (37 °C, 5% CO_2). Medium was then removed and probe LUF8019 or LUF8023 (final concentration: 100 nM) or 1% DMSO (vehicle) in HBSS was added, followed by incubation for 2 h (37 °C, 5% CO_2). HBSS was removed, non-bound probe was washed away with PBS and membranes were prepared as previously reported.[45] Protease inhibitor cocktail (1:100) was added, the membrane fractions were diluted to a concentration of 1 mg/mL and 20 µL was taken per sample. Click mix was freshly prepared by combining 5 parts 100 mM $CuSO_4$, 3 parts 1 M NaAsc, 1 part 100 mM THPTA and 1 part 100 µM Cy5-N_3. 2.22 µL of click mix was added per sample and the samples were incubated for 1 h at rt. 0.5 µL PNGase (5U) was added by which the samples were deglycosylated for 1 h at rt. The samples were denatured by addition of 7.57 µL Laemmli buffer (x4) and incubating for at least 1 h at rt. Samples were then loaded on gel (12.5% acrylamide) and run (180 V, 100 min). Gels were imaged using a Bio-Rad Universal Hood III and in-gel fluorescence. CBB staining was carried out as protein control.

SDS-PAGE data analysis

Gels were analyzed with ImageLab software version 6.0.1 (Bio-Rad). The adjusted volumes of the selected bands were determined using the 'Lane Profile' tab and corrected for the amount of protein per lane, using the adjusted total lane volumes of the CBB stained gels. The adjusted volume of the band at 55 kDa in the molecular weight marker (Pageruler prestained protein ladder) was set to 100% and the other bands were normalized to this value. Further data analysis was carried out using Graphpad Prism. All given percentages are the mean values ± SEM of three individual experiments. Statistical analysis was performed using a one- or two-way ANOVA test with multiple comparisons.

Author Contributions

V.A. synthesized compounds. R.L. performed radioligand displacement experiments. B.L.H.B. and V.A. performed SDS-PAGE experiments. L.H.H., A.P.IJ. and D.v.d.E. supervised the project.

References

[1] B. B. Fredholm, A. P. IJzerman, K. A. Jacobson, K.-N. Klotz, J. Linden, *Pharmacol Rev* **2001**, *53*, 527–552.

[2] A. P. IJzerman, K. A. Jacobson, C. E. Müller, B. N. Cronstein, R. A. Cunha, *Pharmacol Rev* **2022**, *74*, 340–372.

[3] C. Cekic, J. Linden, *Nat Rev Immunol* **2016**, *16*, 177–192.

[4] Z. G. Gao, K. A. Jacobson, *Int J Mol Sci* **2019**, *20*, 5139.

[5] B. Allard, D. Allard, L. Buisseret, J. Stagg, *Nat Rev Clin Oncol* **2020**, *17*, 611–629.

[6] V.-P. Jaakola, M. T. Griffith, M. A. Hanson, V. Cherezov, E. Y. T. Chien, J. R. Lane, A. P. IJzerman, R. C. Stevens, *Science (1979)* **2008**, *322*, 1211–1217.

[7] Y. Chen, J. Zhang, Y. Weng, Y. Xu, W. Lu, W. Liu, M. Liu, T. Hua, G. Song, *Sci Adv* **2022**, *8*, eadd3709.

[8] H. Cai, Y. Xu, S. Guo, X. He, J. Sun, X. Li, C. Li, W. Yin, X. Cheng, H. Jiang, H. E. Xu, X. Xie, Y. Jiang, *Cell Discov* **2022**, *8*, 140.

[9] D. Petroni, C. Giacomelli, S. Taliani, E. Barresi, M. Robello, S. Daniele, A. Bartoli, S. Burchielli, S. Pardini, P. A. Salvadori, F. da Settimo, C. Martini, M. L. Trincavelli, L. Menichetti, *Nucl Med Biol* **2016**, *43*, 309–317.

[10] M. Lindemann, S. Hinz, W. Deuther-Conrad, V. Namasivayam, S. Dukic-Stefanovic, R. Teodoro, M. Toussaint, M. Kranz, C. Juhl, J. Steinbach, P. Brust, C. E. Müller, B. Wenzel, *Bioorg Med Chem* **2018**, *26*, 4650–4663.

[11] M. Lindemann, R. P. Moldovan, S. Hinz, W. Deuther-Conrad, D. Gündel, S. Dukic-Stefanovic, M. Toussaint, R. Teodoro, C. Juhl, J. Steinbach, P. Brust, C. E. Müller, B. Wenzel, *Int J Mol Sci* **2020**, *21*, 3197.

[12] M. Köse, S. Gollos, T. Karcz, A. Fiene, F. Heisig, A. Behrenswerth, K. Kieć-Kononowicz, V. Namasivayam, C. E. Müller, *J Med Chem* **2018**, *61*, 4301–4316.

[13] E. Barresi, C. Giacomelli, S. Daniele, I. Tonazzini, M. Robello, S. Salerno, I. Piano, B. Cosimelli, G. Greco, F. da Settimo, C. Martini, M. L. Trincavelli, S. Taliani, *Bioorg Med Chem* **2018**, *26*, 5885–5895.

[14] J. Barbazán, M. Majellaro, A. L. Martínez, J. M. Brea, E. Sotelo, M. Abal, *Biomedicine and Pharmacotherapy* **2022**, *153*, 113408.

[15] B. L. H. Beerkens, X. Wang, M. Avgeropoulou, L. N. Adistia, J. P. D. van Veldhoven, W. Jespers, R. Liu, L. H. Heitman, A. P. IJzerman, D. van der Es, *RSC Med Chem* **2022**, *13*, 850–856.

[16] A. Temirak, J. G. Schlegel, J. H. Voss, V. J. Vaaßen, C. Vielmuth, T. Claff, C. E. Müller, *Molecules* **2022**, *27*, 3792.

[17] D. Weichert, P. Gmeiner, *ACS Chem Biol* **2015**, *10*, 1376–1386.

[18] Y. Wu, B. Zhang, H. Xu, M. He, X. Deng, L. Zhang, Q. Dang, J. Fan, Y. Guan, X. Peng, W. Sun, *Coord Chem Rev* **2023**, *480*, 215040.

[19] L. Dahl, I. B. Kotliar, A. Bendes, T. Dodig-Crnković, S. Fromm, A. Elofsson, M. Uhlén, T. P. Sakmar, J. M. Schwenk, *bioRxiv* **2022**, 2022.11.24.517810.

[20] B. L. H. Beerkens, Ç. Koç, R. Liu, B. I. Florea, S. E. Le Dévédec, L. H. Heitman, A. P. IJzerman, D. van der Es, *ACS Chem Biol* **2022**, *17*, 3131–3139.

[21] X. Yang, T. J. M. Michiels, C. de Jong, M. Soethoudt, N. Dekker, E. Gordon, M. van der Stelt, L. H. Heitman, D. van der Es, A. P. IJzerman, *J Med Chem* **2018**, *61*, 7892–7901.

[22] B. L. H. Beerkens, I. M. Snijders, J. Snoeck, R. Liu, A. T. J. Tool, S. E. Le Dévédec, W. Jespers, T. W. Kuijpers, G. J. P. van Westen, L. H. Heitman, A. P. IJzerman, D. van der Es, *ChemRxiv* **2023**, DOI 10.26434/chemrxiv-2023-6g59z.

[23] S. Tsukiji, M. Miyagawa, Y. Takaoka, T. Tamura, I. Hamachi, *Nat Chem Biol* **2009**, *5*, 341–343.

[24] S. H. Fujishima, R. Yasui, T. Miki, A. Ojida, I. Hamachi, *J Am Chem Soc* **2012**, *134*, 3961–3964.

[25] T. Tamura, T. Ueda, T. Goto, T. Tsukidate, Y. Shapira, Y. Nishikawa, A. Fujisawa, I. Hamachi, *Nat Commun* **2018**, *9*, 1870.

[26] G. Tomasello, I. Armenia, G. Molla, *Bioinformatics* **2020**, *36*, 2909–2911.

[27] T. Miki, S. H. Fujishima, K. Komatsu, K. Kuwata, S. Kiyonaka, I. Hamachi, *Chem Biol* **2014**, *21*, 1013–1022.

[28] S. M. Moss, P. S. Jayasekara, S. Paoletta, Z. G. Gao, K. A. Jacobson, *ACS Med Chem Lett* **2014**, *5*, 1043–1048.

[29] L. A. Stoddart, N. D. Kindon, O. Otun, C. R. Harwood, F. Patera, D. B. Veprintsev, J. Woolard, S. J. Briddon, H. A. Franks, S. J. Hill, B. Kellam, *Commun Biol* **2020**, *3*, 722.

[30] H. Nonaka, S. Sakamoto, K. Shiraiwa, M. Ishikawa, T. Tamura, K. Okuno, S. Kiyonaka, E. A. Susaki, C. Shimizu, H. R. Ueda, W. Kakegawa, I. Arai, M. Yuzaki, I. Hamachi, *bioRxiv* **2023**, 2023.01.16.524180.

[31] S. Arttamangkul, A. Plazek, E. J. Platt, H. Jin, T. F. Murray, W. T. Birdsong, K. C. Rice, D. L. Farrens, J. T. Williams, *Elife* **2019**, *8*, e49319.

[32] M. Kosar, D. A. Sykes, A. E. G. Viray,] Rosa, M. Vitale, R. C. Sarott, R. L. Ganzoni, D. Onion, J. M. Tobias, P. Leippe, C. Ullmer, E. A. Zirwes, W. Guba, U. Grether, J. A. Frank, D. B. Veprintsev, E. M. Carreira, *ChemRxiv* **2022**, DOI 10.26434/chemrxiv-2022-z58fd.

[33] X. Gómez-Santacana, M. Boutonnet, C. Martínez-Juvés, J. L. Catena, E. Moutin, T. Roux, E. Trinquet, L. Lamarque, J. Perroy, L. Prézeau, J. M. Zwier, J.-P. Pin, A. Llebaria, *ChemRxiv* **2022**, DOI 10.26434/chemrxiv-2022-mqqtz-v2.

[34] D. Xue, L. Ye, J. Zheng, Y. Wu, X. Zhang, Y. Xu, T. Li, R. C. Stevens, F. Xu, M. Zhuang, S. Zhao, F. Zhao, H. Tao, *Org Biomol Chem* **2019**, *17*, 6136–6142.

[35] C. W. Tornøe, C. Christensen, M. Meldal, *Journal of Organic Chemistry* **2002**, *67*, 3057–3064.

[36] V. V. Rostovtsev, L. G. Green, V. V. Fokin, K. B. Sharpless, *Angew. Chem. Int. Ed.* **2002**, *41*, 2596–2599.

[37] C. E. Müller, J. Sandoval-Ramirez, *Synthesis (Stuttg)* **1995**, 1295–1299.

[38] C. E. Müller, D. Shi, M. Manning, J. W. Daly, *J. Med. Chem* **1993**, *36*, 3341–3349.

[39] X. Yang, J. P. D. van Veldhoven, J. Offringa, B. J. Kuiper, E. B. Lenselink, L. H. Heitman, D. van der Es, A. P. IJzerman, *J Med Chem* **2019**, *62*, 3539–3552.

[40] R. Liu, N. J. A. Groenewoud, M. C. Peeters, E. B. Lenselink, A. P. IJzerman, *Purinergic Signal* **2014**, *10*, 441–453.

[41] R. Liu, D. Nahon, B. le Roy, E. B. Lenselink, A. P. IJzerman, *Biochem Pharmacol* **2015**, *95*, 290–300.

[42] X. Wang, W. Jespers, B. J. Bongers, M. C. C. Habben Jansen, C. M. Stangenberger, M. A. Dilweg, H. Gutiérrez-de-Terán, A. P. IJzerman, L. H. Heitman, G. J. P. van Westen, *Eur J Pharmacol* **2020**, *880*, 173126.
[43] S. Hinz, S. K. Lacher, B. F. Seibt, C. E. Müller, *Journal of Pharmacology and Experimental Therapeutics* **2014**, *349*, 427–436.
[44] A. M. Hayallah, J. Sandoval-Ramírez, U. Reith, U. Schobert, B. Preiss, B. Schumacher, J. W. Daly, C. E. Müller, *J Med Chem* **2002**, *45*, 1500–1510.
[45] T. Amelia, J. P. D. Van Veldhoven, M. Falsini, R. Liu, L. H. Heitman, G. J. P. Van Westen, E. Segala, G. Verdon, R. K. Y. Cheng, R. M. Cooke, D. Van Der Es, A. P. IJzerman, *J Med Chem* **2021**, *64*, 3827–3842.
[46] C. Yung-Chi, W. H. Prusoff, *Biochem Pharmacol* **1973**, *22*, 3099–3108.
[47] A. Kourounakis, C. Visser, M. de Groote, A. P. IJzerman, *Biochem Pharmacol* **2001**, *61*, 137–144.
[48] A. Vlachodimou, H. de Vries, M. Pasoli, M. Goudswaard, S.-A. Kim, Y.-C. Kim, M. Scortichini, M. Marshall, J. Linden, L. H. Heitman, K. A. Jacobson, A. P. IJzerman, *Biochem Pharmacol* **2022**, *200*, 115027.